Experimental Validation of a Novel Multistatic Toroidal Reflector Nearfield Imaging System for Concealed Threat Detection

Mohammad.H Nemati, Spiros Mantzavinos, Dan Busuioc, Nicholas Pelepchan, Thurston Brevett, Jacob Londa, Nikhil Phatak, Daniel Castle, Carey M. Rappaport,
ALERT Center of Excellence, Northeastern University, Boston MA, USA, rappaport@neu.edu

***Abstract* – This paper presents the experimental results for a multistatic millimeter wave synthetic aperture radar (SAR) imaging radar for person security screening applications. By making use of an elliptical toroidal antenna, together with a low-cost, highly integrated, wide-bandwidth 57-64 GHz transceiver chipset, a multistatic imaging system is realized which simplifies the 3D imaging system to a less computationally intense 2D problem. The experimental data is in good agreement with the computed data, imaging not only conventional objects, but also challenging targets such as penetrable dielectrics and dihedrals.**

***Key words* — Imaging Systems, Multistatic radar system, Security scanning.**

I. INTRODUCTION

Millimeter-wave imaging systems are becoming prevalent for security applications where noninvasive imaging techniques are required to detect concealed objects. In the 57-64 GHz frequency range the human body acts like a PEC, where the incident waves are totally reflected by the skin. Unlike x-rays, mm-waves are not ionizing.

Nearfield imaging is performed by illuminating the human body target with mm waves and measuring the scattered field. The shape of a human subject is reconstructed by processing the measured field using conventional image reconstruction techniques, such as the inverse source method [1]. The multistatic radar configuration presented here not only is capable of detecting nonmetallic object such as plastic and possibly explosive materials, but also solves the problem of detecting dihedral artifacts from different sections of the human body, which is the main drawback of current monostatic scanning systems in airports [2].

The radar system proposed here is a simple, low-cost, highly integrated and high accuracy imaging solution. The antenna system is a high gain toroidal reflector antenna (Fig. 1) which makes it possible to have a high-resolution imaging system instead of using a dense 2D complex array antenna configuration [3]. The reflector antenna is elliptical in elevation and circular in azimuth, creating a sharp beam in elevation and a wide collimated beam in azimuth. This simplifies the 3D imaging into a set of 2D problems. The 3D image can be simply constructed by stacking the 2D images from different slices. The integrated hardware implementation including the transceiver chipset, FPGA, and digitizer. are described in previous work [4]. This paper will concentrate on the system calibration and measurement results.

This work is supported by Northeastern University's ALERT Center; funded by the Science and Technology Directorate, U.S. Department of Homeland Security under the Award Number 2013-ST-061-ED0001

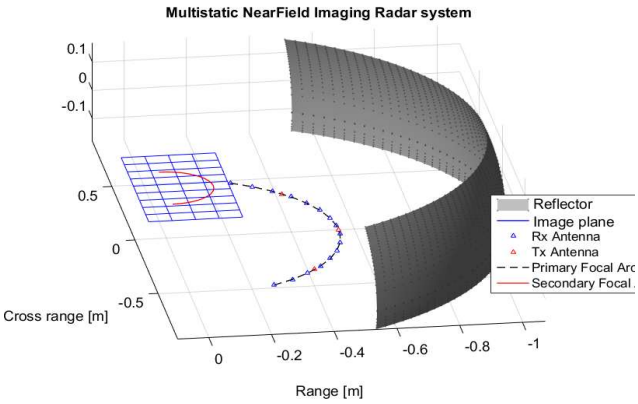

Figure 1: High gain elliptical toroidal reflector geometry, with radius 106 cm, and height 30 cm

II. IMAGING ALGORITHM AND FEED CALIBRATION

An algorithm used for SAR image reconstruction is based on solving the matrix equation $\mathbf{Ax} = \mathbf{b}$ where $\mathbf{b}$ is the column matrix of measured field values, and $\mathbf{A}$ is the matrix representing the field that would be received by the receiving element from an imaginary ideal point scatterer in the image plane, illuminated by a given transmitter. The image $\mathbf{x}$ results from multiplying both sides of the equation by the adjoint (conjugate transpose) matrix $\mathbf{A}^a$, and approximating $\mathbf{A}^a\,\mathbf{A} \sim \mathbf{I}$. In effect, this SAR algorithm removes the phase associated with the ray paths from each transmitter to a given image point to each receiver, and if the image point was indeed on part of the scatter, that image point would have constructive addition for all path combinations, and a bright high intensity spot would appear on the image plane. For the reflector antenna, the $\mathbf{A}$ matrix includes the path from feed element to reflector, then to the target, and back to reflector and receiving feed. Physical optics is used to compute the reflected field.

For best reflector focusing, the transmitter and receiver reflector feed elements need to be placed in the reflector's primary focal arc with millimeter accuracy. The feed position calibration is first done mechanically and then electronically. The electronic calibration optimizes the feed position by plotting field intensity at the image domain. Fig. 2 shows the measured reflector beam intensity plot after the feed position calibration for a transmitting feed element. The plot shows a well-focused beam in elevation and a wide and uniform beam in the cross-range direction, which can be applied to illuminate a very narrow section of the human target.

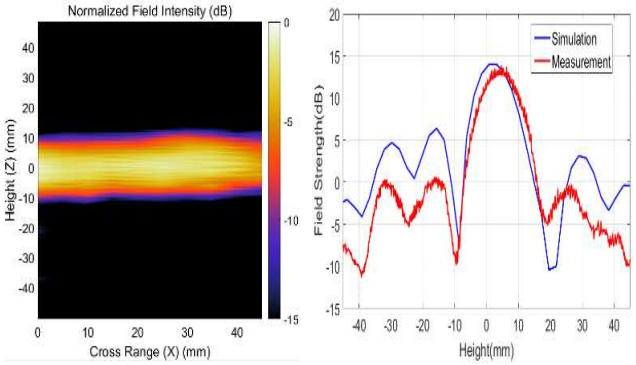

(a) (b)

Figure 2: Field intensity plot at the image domain (a) 2D plot in cross range and height (b) 1D plot in height

III. IMAGING RESULTS

This section presents the reconstructed images for various targets after processing the measured data. The measurement setup has two transmitters at -50 and 50 degrees with a receiver moving along the primary focal arc concentric with the toroidal reflector and with 55 cm radius from -42.5 to 42.5 degrees using a motor. Fig. 3 shows 2D imaging based on the SAR algorithm above for various targets. These images each represent a 2D slice of the middle of the respective targets as seem from above, so the y-axis is range, and the x-axis is cross range, with the illumination coming from below. Among them is the target with a dihedral effect (Fig. 3a), which is perfectly imaged by the radar system. This is a great advantage over the current monostatic radar systems current deployed in airports, which image a dihedral inaccurately as a point retro-reflector. Adjacent body parts and folds of skin scatter much more strongly with monostatic radar, resulting in false alarms. The multistatic configuration clearly prevents retro-reflection and significantly reduces false alarms.

Fig. 3b and 3c show the images for the metal box with a metal bar and a wax-base dielectric explosive simulant.Fig. 3d show the reconstruction of an air duct torso simulant. The incident field on the surface of metallic objects reflects from the front surface, and the reconstructed images shows the corresponding surface contour.

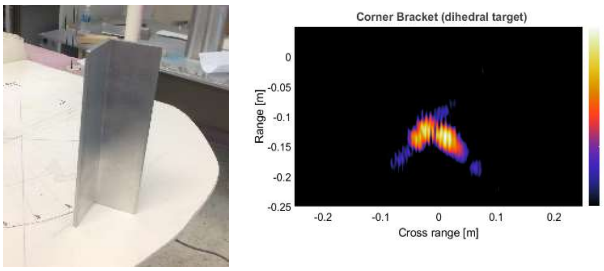

a) Cornerbracket (target with dihedral effect)

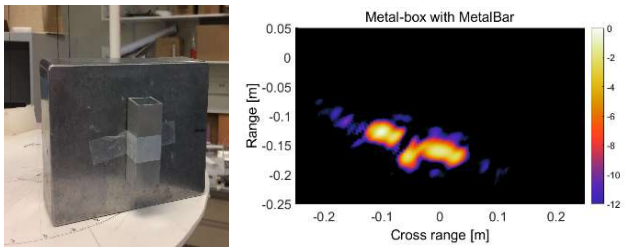

b) Flat metal box with metal bar on front surface

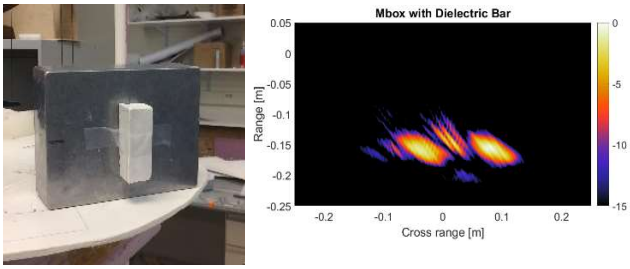

c) Flat metal box with dielectric explosive simulant on front surface

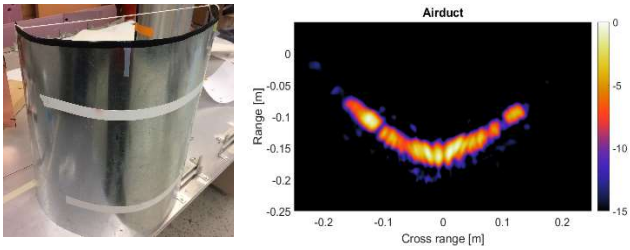

d) Airduct torso simulant

Figure 3: Reconstructed images for various targets based on measured data. The y-axis is range, and x-axis is cross range.

Fig. 3 c shows the same metal box with a dielectric bar with dielectric constant 2.9, which is very close to the dielectric constant of explosive materials. The incident wave propagates more slowly in the dielectric region than in free space before it reaches the metal on the back surface of the dielectric slab, which results in a delay for the reflected wave from the metal surface. Thus, waves will experience more delay in the

dielectric region compared to bare metal the, and the resulting image will appear to be a depression in the metal surface.

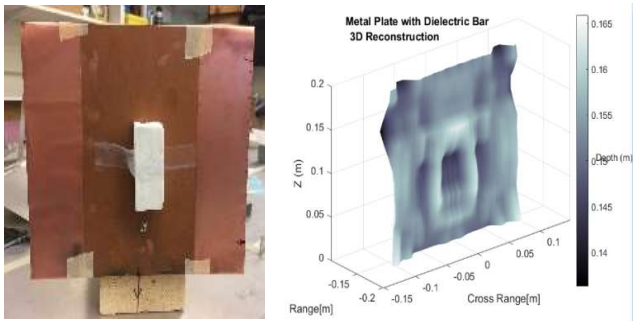

a) **Metal plate with dielectric *bar***

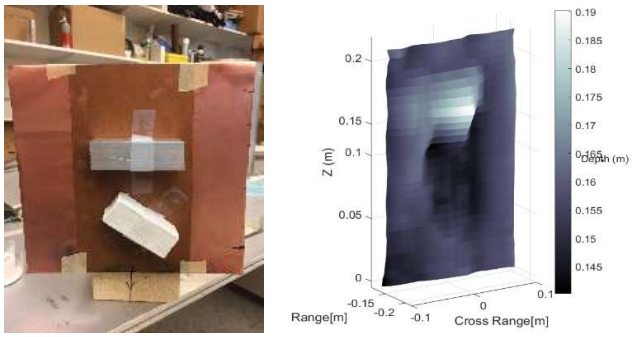

b) **Metal plate with metal bar and dielectric bar**

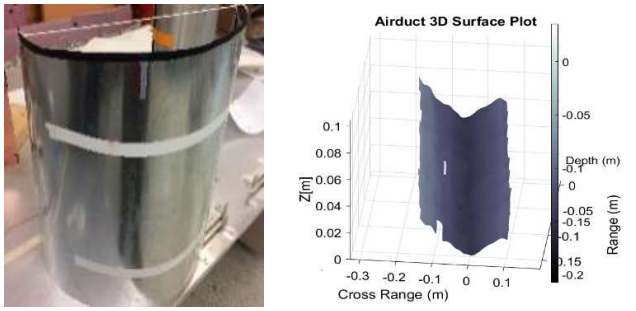

c) **Airduct**

Figure 4: Reconstructed 3D images for various targets based on measured data

Stacking 2D images of different reconstructed slices will result in a 3D surface reconstruction of the target. Fig: 4 shows 3D surface reconstructions of 3 different targets. The images are plotted based on the range position of the maximum reflectivity for each cross range point. The color scale represents depth, lighter being closer to the front of the target, and darker towards the back. As seen in Figs. 3a and 3b, a cavity forms wherever the dielectric is placed on the metal plate. This is due to the same propagation delay that was discussed in the previous paragraph.

IV. CONCLUTIONS

Imaging results based on measured data are presented for the proposed novel multistatic radar system. The results are promising, especially in the cases with targets containing dihedral and dielectric effects. The multistatic system is able to perfectly image a 2D slice of a dihedral target, which has significant computational advantages over the current monostatic system used in most airports. Targets with protruding weak dielectrics can also be identified, as the dielectric creates a propagation delay to the incident wave, making a cavity in the surface of the target. These results further recognize the validity of the multistatic imaging system to detect concealed threats.

REFERENCES

[1] Pastorino, M., A. Massa, and S. Caorsi, "A microwave inverse scattering technique for image reconstruction based on a genetic algorithm," IEEE Trans. Instr. and Meas., Vol. 49, No. 3, 573– 578, Jun. 2000.

[2] Sheen, D. M., D. L. McMakin, and T. E. Hall, "Three-dimensional millimeter-wave imaging for concealed weapon detection," IEEE Transactions on Microwave Theory and Techniques, Vol. 49, No. 9, 1581–1592, Sep. 2001.

[3] Rappaport, Carey M., and Borja Gonzalez-Valdes. "Multistatic nearfield imaging radar for portal security systems using a high gain toroidal reflector antenna." Antennas and Propagation (EuCAP), 2015 9th European Conference on. IEEE, 2015.

[4] Mantzavinos, Spiros, et al. "Low-cost, fused millimeter-wave and 3D point cloud imaging for concealed threat detection." Antennas and Propagation Society International Symposium (APSURSI), 2013 IEEE. IEEE, 2013.

[5] Spiros Mantzavinos, Borja Gonzalez-Valdes, Dan Busuioc, Ryan Miller, Jose A. Martinez-Lorenzo, Carey M , "Low-Cost, Fused Millimeter-Wave and 3D Point Cloud Imaging for Concealed Threat Detection.